Journal of Southeast University (English Edition) Vol. 31, No. 4, pp. 572 - 576 Dec. 2015 ISSN 1003—7985

Numerical simulation of diffusion process for oxidative dehydrogenation of butene to butadiene

Huang Kai Lin Sheng Zhou Jiancheng

(School of Chemistry and Chemical Engineering, Southeast University, Nanjing 211189, China)

Abstract: A comprehensive single particle model which includes the mesoscale and microscale models was developed to study the influence of particle diameter on mass and heat transfer occurring within a ferrite catalyst during the oxidative dehydrogenation of butene to butadiene process. The verified model can be used to investigate the influence of catalyst diameter on the flow distribution inside the particle. The simulation results demonstrate that the mass fraction gradients of all species, temperature gradient and pressure gradient increase with the increase of the particle diameter. It means that there is a high intraparticle transfer resistance and strong diffusion when applying the large catalysts. The external particle mass transfer resistance is nearly constant under different particle diameters so that the effect of particle diameter at external diffusion can be ignored. A large particle diameter can lead to a high surface temperature, which indicates the external heat transfer resistance. Moreover, the selectivity of reaction may be changed with a variety of particle diameters so that choosing appropriate particle size can enhance the production of butadiene and optimize the reaction process.

Key words: multi-scale model; mass and heat transfer; particle diameter; oxidative dehydrogenation of butene to butadiene; single particle model; transfer resistance

doi: 10.3969/j.issn.1003 - 7985.2015.04.024

The requirement of butadiene has increased recently because it is an important raw material for manufacturing a large number of chemical products in the petrochemical industries[1]. Although the production of butadiene primarily depends on the extraction of butadiene from crude C4 stream, establishing as additional cracking unit of naphtha cannot meet the rising demand due to the fact that other basic fractions are excessively produced[2]. The oxidative dehydrogenation of butene has attracted much attention as a promising process to produce butadiene. A great number of catalysts such as vanadium-containing catalyst[3], ferrite-type catalyst[4], Bi-Mo based catalyst[1], and Octahedral Molecular Sieves catalyst[5] have been investigated for this reaction system. As Zinc ferrite is the most efficient catalyst, it has been widely employed by researchers[6].

It is well known that diffusion exists within the catalyst particle. Zinc ferrite and its kinetics have been widely studied for the oxidative dehydrogenation of butene to butadiene, but to the best of our knowledge, no paper reports the influence of the catalyst particle diameter on particle mass and heat transfers[6]. Therefore, a model should be developed to study the effect of the diameter.

In this work, a comprehensive single particle model, containing the mass, energy, and momentum balances as well as the gas-state equations, kinetic equations, and multicomponent diffusion equations, is developed to analyze the process of ODOBTB. The single particle model is a multiscale model, which can study the diffusion on the mesoscale and microscale. In addition, the multiscale model can compute the distribution of pressure, species fractions, and temperature so that the influence of particle size to particle transfer can be achieved.

1 Single Particle Model and Solution Derivation

1.1 Modeling of particle mass and heat transfer

A comprehensive single particle model contains the mass, energy, and momentum balances as well as the gas-state equations, kinetic equations, and multicomponent diffusion equations[7]. After modeling, three assumptions have been accepted: 1) The Zinc ferrite catalyst is regarded as a spherical particle; 2) The deformation of particle can be ignored; and 3) All particle parameters vary with the radial position only. Thus, the following model equations can be obtained.

Total mass balance in a particle:

$$\varepsilon \frac{\partial \rho_{\mathrm{g}}}{\partial t} + \frac{v_{\mathrm{r}}^{\mathrm{s}}}{r^2} \frac{\partial}{\partial r}(r^2 \rho_{\mathrm{g}}) = 0 \tag{1}$$

Momentum balance in a particle:

$$v_{\mathrm{r}} = \frac{\varepsilon d_0^2}{32\tau\mu} \frac{\partial P}{\partial r} \tag{2}$$

Component material balance in a particle:

$$\varepsilon \frac{\partial}{\partial t}(\rho Y)_i + \frac{v_{\mathrm{r}}^{\mathrm{s}}}{r^2} \frac{\partial}{\partial r}(r^2 \rho Y_i) = -\frac{1}{r^2} \frac{\partial}{\partial r}(r^2 j_{i,\mathrm{r}}) + \bar{S}_i \tag{3}$$

Received 2015-01-05.

Biography: Huang Kai (1973—), male, doctor, associate professor, huangk@seu.edu.cn.

Foundation items: The National Science Foundation of China (No. 21576049, 21576050), the Fundamental Research Funds for the Central Universities (No. 2242014K10025).

Citation: Huang Kai, Lin Sheng, Zhou Jiancheng. Numerical simulation of diffusion process for oxidative dehydrogenation of butene to butadiene[J]. Journal of Southeast University (English Edition), 2015, 31(4): 572 - 576. [doi: 10.3969/j.issn.1003 - 7985.2015.04.024]

Heat balance in a particle:

$$\left[(1-\varepsilon)\rho_{\mathrm{cat}}C_{\mathrm{p,cat}}+\varepsilon\rho\sum_{i=1}^{n}Y_iC_{\mathrm{p},i}\right]\frac{\partial T}{\partial t}=-\rho\sum_{i=1}^{n}Y_iC_{\mathrm{p},i}v_{\mathrm{r}}^{\mathrm{s}}\frac{\partial T}{\partial t}-\frac{1}{r^2}\frac{\partial}{\partial r}(r^2Q_{\mathrm{r}})+\hat{S} \tag{4}$$

where ε is the catalyst porosity; ρ_{g} is the mixture gas density, kg/m^3; ρ_{cat} is the real catalyst density, kg/m^3; ρ_i is the i-th component density, kg/m^3; P is the pressure, kPa; τ is the curvature factor; d_0 is the catalyst pore diameter, m; $v_{\mathrm{r}}^{\mathrm{s}}$ is the gas velocity at the particle's outer surface, m/s; r is the catalyst particle radial coordinate, m; Y_i is the mass fraction of the i-th component; $j_{i,\mathrm{r}}$ is the mass diffusion flux, kg/(m^2 · s); S_i is the mass source of the i-th component of the single model, kg/(m^3 · s); $C_{\mathrm{p,cat}}$ is the mass heat capacity of the catalyst, kJ/(kg · K); $C_{\mathrm{p},i}$ is the mass heat capacity of the i-th component, kJ/(kg · K); Q_{r} is the heat flux, J/(m^2 · s); T is the temperature, K; $\hat{S}$ is the heat source of the single model, J/(m^3 · s). The above parameters can be calculated via the next boundary conditions:

When $r=0$,

$$j_{i,0}=0,\ Q_{\mathrm{r}}=0 \tag{5}$$

When $r=\dfrac{d_{\mathrm{p}}}{2}$,

$$-k_{i,\mathrm{g}}(\rho_i^{\mathrm{b}}-Y_i\rho^{\mathrm{s}})=j_{i,\mathrm{s}}+v_{\mathrm{r}}^{\mathrm{s}}\rho Y_i,\ Q_{\mathrm{r}}+\rho Cp_{\mathrm{s}}Tv_{\mathrm{r}}^{\mathrm{s}}=-h_{i,\mathrm{g}}(T^{\mathrm{b}}-T^{\mathrm{s}}) \tag{6}$$

where $k_{i,\mathrm{g}}$ is the mass transfer coefficient, W/(s · K); $h_{i,\mathrm{g}}$ is the heat transfer coefficient, W/(m^2 · K), and they can be computed via the next equations:

$$k_{i,\mathrm{g}}=\frac{D_{i,\mathrm{m}}Sh_i}{d_{\mathrm{p}}} \tag{7}$$

$$Sh_i=2+0.6Sc^{1/3}Re_i^{0.5}\frac{\mu_i}{\rho_iD_{i,\mathrm{m}}} \tag{8}$$

$$Sc_i=\frac{\mu_i}{\rho_iD_{i,\mathrm{m}}} \tag{9}$$

$$Re_i=\frac{d_{\mathrm{p}}u\rho_i}{\mu_i} \tag{10}$$

$$h_{i,\mathrm{g}}=\frac{k_{i,\mathrm{g}}Nu_i}{d_{\mathrm{p}}} \tag{11}$$

$$Nu_i=2+0.6Pr^{1/3}Re^{0.5} \tag{12}$$

$$Pr=\frac{C_{\mathrm{p},i}\mu_i}{\lambda_i} \tag{13}$$

where d_{p} is the catalyst average diameter, m; Sh_i is the Sherwood number of the i-th component; Sc is the Schmidt number; Pr is the Prandtl number; Re is the Reynolds number; f is the fanning coefficient; μ is the mixture fluid viscosity, Pa/s; u is the apparent gas velocity, m/s.

1.2 Reaction kinetics

A kinetics model derived by Ding et al.[8] is used to describe the ODOBTB process based on the Mars-van Krevelen mechanism. The kinetics equations are shown as follows:

$$\mathrm{C_4H_8}+\frac{1}{2}\mathrm{O_2}\xrightarrow{r_1}\mathrm{C_4H_6}+\mathrm{H_2O}$$

$$r_1=\frac{k_1P_{\mathrm{C_4H_8}}k_0P_{\mathrm{O}}}{(k_1+k_2)P_{\mathrm{C_4H_8}}+k_3P_{\mathrm{C_4H_6}}+k_0P_{\mathrm{O}}} \tag{14}$$

$$\mathrm{C_4H_8}+6\mathrm{O_2}\xrightarrow{r_2}4\mathrm{CO_2}+4\mathrm{H_2O}$$

$$r_2=\frac{k_2P_{\mathrm{C_4H_8}}k_0P_{\mathrm{O}}}{(k_1+k_2)P_{\mathrm{C_4H_8}}+k_3P_{\mathrm{C_4H_6}}+k_0P_{\mathrm{O}}} \tag{15}$$

$$\mathrm{C_4H_6}+\frac{11}{2}\mathrm{O_2}\xrightarrow{r_3}4\mathrm{CO_2}+3\mathrm{H_2O}$$

$$r_3=\frac{k_3P_{\mathrm{C_4H_6}}k_0P_{\mathrm{O}}}{(k_1+k_2)P_{\mathrm{C_4H_8}}+k_3P_{\mathrm{C_4H_6}}+k_0P_{\mathrm{O}}} \tag{16}$$

$$k_i=A_i\exp\left(\frac{E_{\mathrm{a},i}}{RT}\right) \tag{17}$$

r_1, r_2 and r_3 represent the reaction rates of the chemical equations for Eqs. (14) to (16), respectively. More details about kinetics parameters are listed in Tab. 1[8].

Tab. 1 Kinetic parameters for kinetic model

Reactions	A_i	$E_{\mathrm{a},i}$/(kJ · mol^{-1})	ΔH_{r}/(kJ · mol^{-1})
1	$1.148\,6\times10^{10}$	$1.398\,39\times10^{5}$	−128.1
2	2.378×10^{5}	$8.708\,54\times10^{4}$	−2 552.6
3	2.378×10^{5}	$8.708\,54\times10^{4}$	−2 394.5

1.3 Solution derivation

The above equations are discretized by the orthogonal collocation method and then the equations can be converted into a set of differential equations. The ODE23S function in the Matlab soft is utilized to compute these differential equations. The model solution and the relationship of the sub-model are shown in Fig. 1. All the simulations are performed on a workstation with four

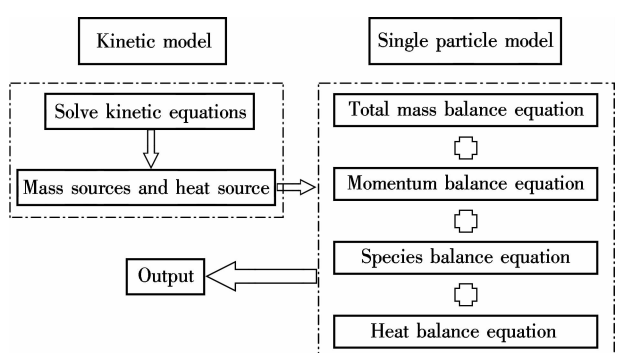

Fig. 1 The whole flow-sheet for solving the single model

4.10 GHz Pentium CPUs and 8 GB memory. Modeling with 3, 4, 6, 8, and 10 points are first executed to confirm whether the results are dependent on the number of collocation points or not. The result is that four points can obtain adequately accurate results. Consequently, the simulations are based on four collocation points. The parameters of simulation are listed in Tab. 2[9-12].

Tab. 2 The parameters for the model

Parameters	Value
Bulk pressure/kPa	100
Bulk temperature/K	593
Catalyst density/($kg \cdot m^{-3}$)	1 919
Particle conductivity/($W \cdot (m \cdot K)^{-1}$)	0.251 4
Particle heat capacity	1 580
Particle porosity	0.35
$Y(C_4H_8):Y(O_2):Y(H_2O)$	0.161:0.080 5:0.758 5
Curvature factor	4
Average pore diameter/nm	16.5
Gas velocity/($m \cdot s^{-1}$)	0.033

2 Results and Discussion

2.1 Model validation

In order to validate the model, the effectiveness factor between the simulation and experiment are compared based on the butene reaction (reaction steps (14) and (15)). The effectiveness factor η can be calculated by

$$\eta = \frac{\text{Actual rate of reaction}}{\text{Rate of reaction with surface condition}} \quad (18)$$

As shown in Fig. 2, the experimental data and simulated data are similar, indicating that the model is valid. Therefore, the model can effectively predict the effect of particle diameter to diffusion.

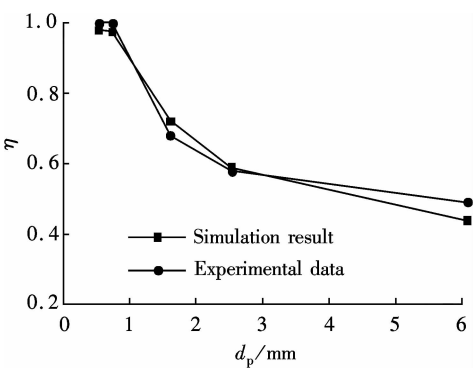

Fig. 2 The comparison between simulation result and experimental data

2.2 Effect of particle diameter to particle transfer

The single model was validated in the above section. Thus, it can be used to study the distribution of pressure, species concentration, and temperature along a radial direction when changing particle diameter.

2.2.1 Distribution of species concentration

Fig. 3 depicts that the species concentration gradient increases with the increase of the catalyst diameter. When

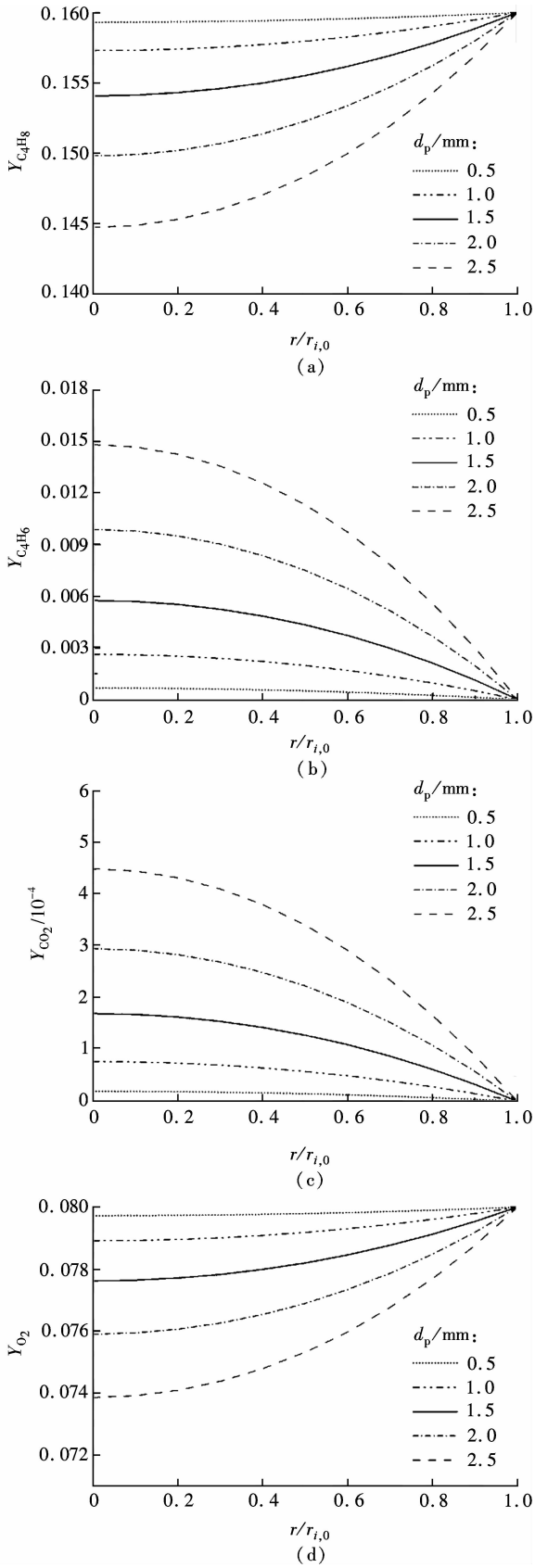

Fig. 3 Effect of the particle diameter on the intraparticle species mass fraction along the radial direction

$d_p < 0.5$ mm, the gradient can be ignored, which shows the intraparticle mass transfer resistance can be considered to be zero. According to the component material balance in a particle (see Eq. (3)), the mass fractions of species are primarily determined via the mass source term $\bar{S}_i$ and the mass diffusion flux $j_{i,r}$. It is found that $\bar{S}_i$ and $j_{i,r}$ have negative and positive effects on the C_4H_8 mass fraction. The mass transfer resistance increases when using a large catalyst and it is more difficult for butene to transfer into the particle, which causes a more obvious intraparticle fraction gradient. The mass fraction of every species at surface is similar with different catalyst diameters, which means that the external mass transfer resistance is hardly related to particle size. A high *Re* leads to a great $k_{i,g}$ on the basis of Eq. (10). Besides, $k_{i,g}$ varies inversely with the catalyst diameter according to Eq. (7). Therefore, the catalyst diameter has no effect on $k_{i,g}$, namely the external mass transfer resistance. Furthermore, the changing degree of the species gradient is different with the varying particle size in Fig. 3. For example, when the catalyst diameter increases from 0.5 to 2.5 mm, the mass fraction of butadiene increases from 6.65×10^{-4} to 1.48×10^{-2}, while carbon dioxide increases from 1.93×10^{-5} to 4.51×10^{-4}. The changing of butadiene is larger than that of carbon dioxide with varying catalyst size. It reveals that the effect of the particle diameter is also related to the selectivity of ODOBTB reaction.

2.2.2 Distribution of temperature

Fig. 4 describes the changing of the intraparticle temperature with the particle size. Inside the catalyst, a low Q_r and a high $\hat{S}$ together cause a high temperature, which implies that the heat transfer resistance increases with the increase of particle size. In addition, the surface temperature increases with the increase of diameter because $h_{i,g}$ decreases with the increase of particle size.

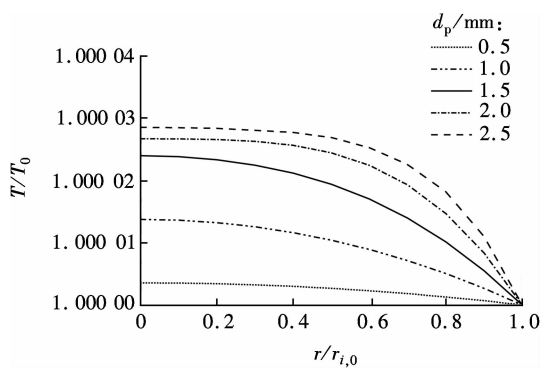

Fig. 4 Effect of particle diameter on the intraparticle temperature along the radial direction

2.2.3 Distribution of pressure

Fig. 5 shows the pressure distribution profiles within the particle along the radial direction at different particle diameters. Under the steady state condition, an ideal gas law is derived as

$$\frac{\partial P}{\partial r} = \frac{2}{r}P + \frac{P}{T}\frac{\partial T}{\partial r} - \frac{P}{M}\frac{\partial M}{\partial r} \tag{19}$$

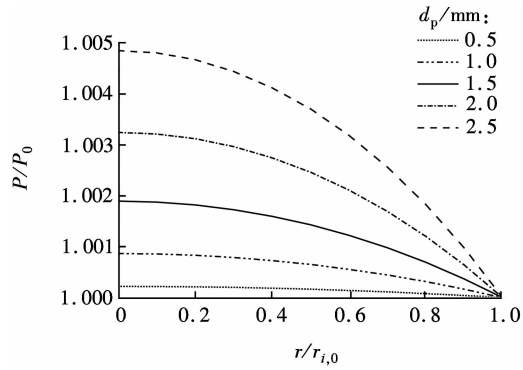

Fig. 5 Effect of particle diameter on the intraparticle pressure along the radial direction

According to Eq. (19), the trend of pressure, temperature, and species concentration should be coincident because $\frac{\partial P}{\partial r}$ is a linear function of both $\frac{\partial T}{\partial r}$ and $\frac{\partial M}{\partial r}$. Therefore, the pressure distribution profiles are similar to those profiles in Figs. 3 and 4.

3 Conclusions

Based on the equations of transfer process, the gas-state equations, kinetic equations and multicomponent diffusion equations, a comprehensive single particle model is established to study the effect of particle diameter on mass and heat transfer occurring within a ferrite catalyst during the ODOBTB reaction process. The simulation demonstrates that the mass fraction gradients of all species, temperature gradient and pressure gradient increase with the increase in the particle diameter. This paper gives new insights into the ODOBTB reaction process. The advanced model can describe the effect of particle diameter after model validation and the conclusions are listed as follows:

1) With the increase in the particle diameter, all species mass fractions gradient, temperature gradient, and pressure gradient increase, which indicates that the transfer resistance increases and an obvious diffusion phenomenon exists with a large particle size.

2) Since the mass transfer coefficient $k_{i,g}$ is a constant, the particle diameter hardly affects external mass transfer resistance. When using a smaller catalyst, the external surface temperature of the particle decreases, suggesting the decrease of external heat transfer resistance.

3) The particle diameter is also related to the selectivity of the ODOBTB reaction. It is of great significance to choose appropriate particle size for enhancing the production of butadiene and optimization of the reaction process.

References

[1] Park J H, Row K, Shin C H. Oxidative dehydrogenation

of 1-butene to1, 3-butadiene over $BiFe_{0.65}Ni_xMo$ oxide catalysts: effect of nickel content [J]. *Catalysis Communications*, 2013, **31**(10): 76 - 80.
[2] Ji C J, Kim H, Choi A S, et al. Effect of pH in the preparation of γ-Bi_2MoO_6 for oxidative dehydrogenation of *n*-butene to 1, 3-butadiene: correlation between catalytic performance and oxygen mobility of γ-Bi_2MoO_6 [J]. *Catalysis Communications*, 2007, **8**(3): 625 - 628.
[3] Cortés I, Rubio O, Herguido J, et al. Kinetics under dynamic conditions of the oxidative dehydrogenation of butane with doped V/MgO [J]. *Catalysis Today*, 2004, **91 - 92**: 281 - 284.
[4] Lee H, Jung J C, Kim H, et al. Preparation of $ZnFe_2O_4$ catalysts by a co-precipitation method using aqueous buffer solution and their catalytic activity for oxidative dehydrogenation of *n*-butene to 1,3-butadiene [J]. *Catalysis Letters*, 2008, **122**(3/4): 281 - 286.
[5] Yin Y G, Xu W Q, DeGuzman R, et al. Studies of stability and reactivity of synthetic cryptomelane-like manganese oxide octahedral molecular sieves [J]. *Inorganic Chemistry*, 1994, **33**(19): 4384 - 4389.
[6] Lee H, Jung J C, Song I K. Oxidative dehydrogenation of *n*-Butene to 1, 3-butadiene over sulfated $ZnFe_2O_4$ catalyst [J]. *Catalysis Letters*, 2009, **133**(3/4): 321 - 327.
[7] Solsvik J, Jakobsen H A. Modeling of multicomponent mass diffusion in porous spherical pellets: application to steam methane reforming and methanol synthesis [J]. *Chemical Engineering Science*, 2011, **66**(9): 1986 - 2000.
[8] Ding X J, Xiao D L, Wang X L, et al. The redox model of the kinetics for the oxidative dehydrogenation over the ferrite catalyst [J]. *Journal of Molecular Catalysis*, 1988, **2**(1): 25 - 30. (in Chinese)
[9] Liu G Z. F-90 ferrite fixed bed catalyst for oxidative dehydrogenation of *n*-Butene to butadiene [J]. *China Synthetic Rubber Industry*, 1991, **14**(3): 179 - 182. (in Chinese)
[10] Jin Y, Yu Q Q, Xu X Q, et al. The effect of intraparticle diffusion on the oxidative dehydrogenation of butane-1 over Fe-Mg-Zn [J]. *Acta Scientiarum Naturalium Universitatis Pekinensis*, 1986, **2**: 29 - 36. (in Chinese)
[11] Jin Y, Yu Q Q, He X C, et al. The effect of intraparticle diffusion on the deep dehydrogenation of butadiene over Fe-Mg-Zn [J]. *Environmental Science*, 1986, **7**(1): 2 - 7. (in Chinese)
[12] Weidenfeller B, Hofer M, Schilling F R. Thermal conductivity, thermal diffusivity, and specific heat capacity of particle filled polypropylene [J]. *Composites Part A: Applied Science and Manufacturing*, 2004, **35**(4): 423 - 429.

丁烯氧化脱氢制丁二烯反应扩散过程的数值模拟

黄 凯 林 生 周建成

(东南大学化学化工学院, 南京 211189)

摘要:为了研究催化剂粒子直径对丁烯催化氧化制丁二烯体系铁酸盐催化剂内外扩散的影响,建立了介观和微观的多尺度模型.将该模型有效化后用来研究催化剂直径对粒子内流场的影响.模拟结果显示:所有组分的质量分数梯度、温度梯度和压力梯度随着粒子直径增大而变大,表明增大粒子直径会使内扩散阻力增大、使内扩散越显著.在不同粒径的催化剂下,组分外扩散传质阻力是一个常数,粒径对粒子组分的外扩散影响不大.随着粒子直径增大,粒子外表面温度增加,即外扩散传热阻力增大.此外,催化剂粒径的变化会影响丁烯催化氧化制丁二烯反应的选择性,选择合适粒径的催化剂能够优化反应过程和提高目标产物丁二烯的产率.

关键词:多尺度模型;传质与传热;粒子直径;丁烯催化氧化制丁二烯;单颗粒模型;扩散阻力
中图分类号:TQ015.9